ARTICLE IN PRESS

Available online at www.sciencedirect.com

ScienceDirect

Proceedings of the Combustion Institute xxx (2010) xxx–xxx

Proceedings of the Combustion Institute

www.elsevier.com/locate/proci

Coupling of in situ adaptive tabulation and dynamic adaptive chemistry: An effective method for solving combustion in engine simulations

Francesco Contino [a,*], Hervé Jeanmart [a], Tommaso Lucchini [b], Gianluca D'Errico [b]

[a] *Université catholique de Louvain, Institute of Mechanics, Materials, and Civil Engineering, Louvain-la-Neuve, Belgium*
[b] *Politecnico di Milano, Dipartimento di Energetica, Milano, Italy*

Abstract

Using detailed mechanisms to include chemical kinetics in computational fluid dynamics simulations is required for many combustion applications, yet the resulting computational cost is often extremely prohibitive. In order to reduce the resources dedicated to this stage, we investigated the coupling of the dynamic adaptive chemistry (DAC) reduction scheme with the in situ adaptive tabulation (ISAT) algorithm. This paper describes the tabulation of dynamic adaptive chemistry (TDAC) method which takes advantage of both ISAT and DAC to reduce the impact of the mesh and the oxidation mechanism on the computational cost, particularly for unsteady applications like internal combustion engines. In the context of homogeneous charge compression ignition (HCCI), we performed simulations on simplified 2D cases using various *n*-heptane mechanisms and on a real case mesh using a detailed 857-species iso-octane mechanism. Compared to the direct integration of the combustion reactions, results are in very good agreements and a speed-up factor above 300 is obtained. This is significantly better than what was reported for ISAT and DAC which illustrates the synergy of the two methods. In addition, an experimental validation has also been performed with low load HCCI data. Accordingly, the TDAC method is a significant improvement for the computation of the combustion chemistry in engine simulations and allows the use of detailed mechanisms with practical case meshes in simulations that are inconceivable using direct integration.

Keywords: In situ adaptive tabulation; Dynamic adaptative chemistry; Homogeneous charge compression ignition; Internal combustion engine; Computational fluid dynamics

1. Introduction

The use of detailed chemistry has become a fundamental prerequisite for realistic computational fluid dynamics (CFD) simulations of the combustion process in internal combustion engines (ICE). Thanks to the comprehensive mechanisms, it is possible to describe the combustion of surrogate fuel mixtures over a wide range of operating conditions, the formation of the main pollutant emissions (soot, NO_x and HC) and the heat release rate under conventional and innovative combustion modes such as PCCI or HCCI [1–3]. When

* Corresponding author. Address: Building Stévin-0, Room b.055, Place du Levant, 2, 1348 Louvain-la-Neuve, Belgium. Fax: +32 (0)10 452692.
E-mail address: francesco.contino@uclouvain.be (F. Contino).

1540-7489/$ - see front matter © 2010 The Combustion Institute. Published by Elsevier Inc. All rights reserved.
doi:10.1016/j.proci.2010.08.002

Please cite this article in press as: F. Contino et al., *Proc. Combust. Inst.* (2010), doi:10.1016/j.proci.2010.08.002

complex chemical mechanisms are included in combustion models, the evolution of the chemical species in each computational cell is performed by an operator-splitting technique, where an ODE stiff solver takes the thermochemical conditions (temperature, pressure and species concentration) and integrates the chemical problem over the time-step, solving the species and the energy equations [4]. However, this technique implies the evaluation of the Jacobian which is computationally demanding when hundreds of species and thousands of reactions are involved, hence limiting the application of detailed kinetics for practical ICE simulations. To reduce the computational efforts, different approaches exist, an overview can be found in [5]. Basically, CPU time reduction can be performed by solution storage and retrieval techniques or by the reduction of the chemical schemes. Several tabulation methods have been developed including, in situ adaptive tabulation (ISAT) [6], piecewise reusable implementation of solution mapping (PRISM) [7] or intrinsic low-dimensional manifold (ILDM) [8], further developed in flame prolongation of ILDM (FPI) [9]. The reduction of the chemical schemes can be performed by skeletal reduction through elimination of species and reactions that have a small contribution to the overall activity of the system. These methods include sensitivity analysis [10], computational singular perturbation (CSP) [11], directed relation graph (DGR) [12], DRG with error propagation (DRGEP) [13] and dynamic adaptive chemistry (DAC) based on DRG and DRGEP [14]. Other techniques could further reduce the resulting skeletal mechanism such as lumping [15], chemistry-guided reduction [16] or quasi steady-state assumptions (QSSA) [17].

Within the framework of ICE simulations, ISAT and DAC have proved to be particularly effective. Their adaptive behavior does not require the preprocessing or pretabulation of sample points which is more effective when a large range of thermochemical conditions is accessed.

Although ISAT and DAC provide a significant reduction of the computational time, the achieved speed-up is still not satisfactory when one of the two approaches is applied in the simulation of ICE. This is due both to mixture inhomogeneities and changes in the thermodynamic conditions during the simulation. The first reduces the number of retrieves that can be used by the ISAT method and the second requires to perform a high number of ODE integrations even if DAC is used. For this reason, the authors propose a new methodology called TDAC (tabulation of dynamic adaptive chemistry) that combines the advantages of ISAT and DAC to solve complex combustion chemistry problems, see Section 2. The proposed approach has been implemented by the authors into the Lib-ICE code, which is a set of libraries and solvers for ICE simulations based on the OpenFOAM® technology [18–20]. The performances of TDAC were firstly evaluated on a simplified geometry using *n*-heptane mechanisms and finally the proposed methodology has been further validated with experimental data of a real HCCI engine, see Section 3.

2. Computational methods

This section first describes the DAC and ISAT methods. Presenting the limits of ISAT, it then proposes a modification to improve the algorithm in ICE conditions. Finally, it discusses the new TDAC method with details on the coupling of DAC and ISAT.

2.1. Dynamic adaptive chemistry

The DAC method computes reduced mechanisms that are valid for the local thermochemical conditions, i.e., it reduces continuously the mechanism instead of preprocessing it [14,21]. In this work, DAC has been extended to full CFD meshes with wall heat transfer.

The reduction algorithm is executed before every call to the stiff solver in each computational cell. It is based on the directed relation graph (DRG) method developed by Lu and Law [22]. It first computes the matrix of the normalized contributions that represents the error on the production and consumption of a species when another is removed from the mechanism. This matrix also represents the strength of the direct link between two species.

Then the algorithm computes the strength of the paths connecting all the species to a user-defined search initiating set of species. In the following simulations, $\{\mathrm{fuel}, \mathrm{CO}, \mathrm{HO_2}\}$ is used as the search initiating set.

In the final step, the reduction scheme removes from the mechanism the species with a value of path strength below a user-defined threshold, $\varepsilon_{\mathrm{DAC}}$, and all the reactions containing at least one disabled species. The ODE associated with these disabled species are not solved, however, their concentration are still considered when evaluating the rate function of the remaining three-body and pressure-dependent reactions. According to the analysis of Liang et al. [14], $\varepsilon_{\mathrm{DAC}}$ is set to 10^{-4} in the following simulations.

The search algorithm originally loops over all species in the mechanism when computing the strength of the paths. Since most of the species are only connected to few others, in the current implementation, it is slightly modified to only evaluate the initialized direct links between species as proposed by Lu and Law [22]. When computing the matrix of contributions, another matrix is then created to store the direct links for each species.

Please cite this article in press as: F. Contino et al., *Proc. Combust. Inst.* (2010), doi:10.1016/j.proci.2010.08.002

2.2. In situ adaptive tabulation

The ISAT algorithm intends to reuse computationally demanding results, e.g. the integration of large and stiff ODE systems, by storing those results and all the data needed to retrieve them.

A thermochemical state is defined by the composition $\psi = \{Y_1, Y_2, \ldots, Y_{N_s}, T, p\}$, where Y_i are the species mass fractions, N_s is the number of species, T is the temperature and p is the pressure. The integration of the reaction equations for a fixed time step Δt maps the initial composition $\psi^0 = \psi(t_0)$ to the reacted value $\psi(t_0 + \Delta t)$ which is a unique function of ψ^0 called the reaction mapping, $\mathbf{R}(\psi^0)$.

The ISAT method stores this reaction mapping for subsequent uses. During computation, given a query point, ψ^q, it computes a linear approximation of the mapping:

$$\mathbf{R}(\psi^q) \approx \mathbf{R}^l(\psi^q) = \mathbf{R}(\psi^0) + \delta\mathbf{R}^l, \tag{1}$$

where $\delta\mathbf{R}^l = \mathbf{A}(\psi^0)(\psi^q - \psi^0)$ and $\mathbf{A}$ is the mapping gradient matrix computed according to the Jacobian of the chemical source term.

The linear approximation defined by Eq. (1) is valid in the region of accuracy (ROA) which is the connected region containing ψ^0 and all the ψ^q respecting the condition on the local error, $\varepsilon_{\text{local}}$:

$$\varepsilon_{\text{local}} = |\mathbf{R}(\psi^q) - \mathbf{R}^l(\psi^q)| = |\delta\mathbf{R} - \delta\mathbf{R}^l| \leqslant \varepsilon_{\text{ISAT}}, \tag{2}$$

where $\varepsilon_{\text{ISAT}}$ is a user-specified tolerance and $\delta\mathbf{R} = \mathbf{R}(\psi^q) - \mathbf{R}(\psi^0)$. Usually, the ROA is not computed according to this definition but is more conveniently approximated by a conservative hyper-ellipsoid in the composition space called ellipsoid of accuracy (EOA):

$$\text{EOA} \equiv \delta\psi^T \widetilde{\mathbf{A}}^T \mathbf{B}^T \mathbf{B} \widetilde{\mathbf{A}} \delta\psi \leqslant \varepsilon_{\text{ISAT}}^2, \tag{3}$$

where $\mathbf{B}$ is an optional scaling matrix, $\widetilde{\mathbf{A}}$ is the modified $\mathbf{A}$ matrix (see [6,23]) and $\delta\psi = \psi^q - \psi^0$.

During the calculation, the table is built up according to the received queries. It consists of a binary tree with leafs and nodes. The leafs store ψ, $\mathbf{R}(\psi)$, $\mathbf{A}(\psi)$ and the EOA description. The nodes stores the hyperplanes in the composition space that allow to scan the binary tree to retrieve the closest stored composition. For each query, one of the following three operations is performed: retrieving, growing or adding. If ψ^q is in the EOA, ISAT retrieves the reaction mapping of ψ^q using Eq. (1). If ψ^q is not in the EOA, the stiff solver is called to compute the direct integration of the reaction equations and ISAT checks the local error using Eq. (2). If this error is less than $\varepsilon_{\text{ISAT}}$, the current approximation of the ROA is too conservative and the EOA is grown to include ψ^q. Otherwise a new leaf is added to the binary tree to store $\mathbf{R}(\psi^q)$. Further details about ISAT can be found in [6].

The current implementation of ISAT also includes some new features introduced by Lu and Pope [23]. The EOA is defined by

$$\text{EOA} \equiv \delta\psi^T \mathbf{L}\mathbf{L}^T \delta\psi \leqslant 1, \tag{4}$$

where $\mathbf{L}$ is the Cholesky factorization of $\widetilde{\mathbf{A}}^T\mathbf{B}^T\mathbf{B}\widetilde{\mathbf{A}}/\varepsilon_{\text{ISAT}}^2$. Taking advantage of this EOA formulation, $\mathbf{L}$ is readily computed from the QR decomposition of $\mathbf{B}\widetilde{\mathbf{A}}/\varepsilon_{\text{ISAT}}$. The use of this matrix is computationally more efficient because the simple triangular matrix–vector multiplication $\|\mathbf{L}^T\delta\psi\| \leqslant 1$ is used to check if a query point lies in the EOA. In addition, the growth process can be done by the rank-one modification algorithm [24] which allows to update the QR decomposition with only $O(N_s^2)$ operations instead of $O(N_s^3)$ [25].

2.3. Modification of ISAT

ISAT is originally developed for constant-pressure and high-temperature chemistry flows and it achieved a particularly good speed-up factor (around 10^3) in the context of particle based probability density function methods for chemically reacting turbulent flows. When a large range of thermochemical conditions is encountered in combustion simulations (ICE, gas turbine burners, etc.), the number of queries resulting in retrieving is smaller and a lot of time is spent in addition and growth with a consequent reduction of the speed-up factor around 10 [6,26]. Therefore, we adapted the ISAT algorithm for this kind of applications by regularly updating the binary tree. These modifications are illustrated here for the ICE case, but they are also valid for the simulation of other combustion systems.

The modification is similar to the periodical clean-up proposed in DOLFA (Database for on-line function approximation [27]). In the present implementation, a stored point is removed from the binary tree according to two user-specified parameters: a number of time steps N_{ms} and a number of growths N_{mg}.

For a moderate value of $\varepsilon_{\text{ISAT}}$, the use of N_{ms} allows to compute more accurately the reaction rate in the pre-ignition phase. Given that a new point is added to the binary tree according to $\varepsilon_{\text{ISAT}}$, a very small value is required to represent the first steps of the combustion. To avoid unnecessary severe tolerance for the main combustion, leading to a substantial increase in the computational time, the stored point is replaced when deemed too old, i.e., after N_{ms} time steps or crank angle degree (CAD).

The growth process is limited by N_{mg} to decrease the total number of growths. In ICE simulations, before and during ignition, the queries are moving toward compositions with high pressure and temperature. This usually leads to distorted EOA where the queries are still within the tolerance, $\varepsilon_{\text{ISAT}}$, but relatively far from the center ψ^0

Please cite this article in press as: F. Contino et al., *Proc. Combust. Inst.* (2010), doi:10.1016/j.proci.2010.08.002

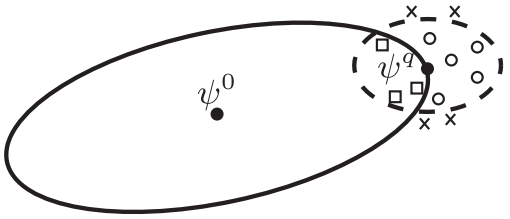

Fig. 1. Instead of distorting the EOA by growing it with ψ^q, the number of retrieves increases when the EOA is replaced after N_{mg} growths by the one centered in ψ^q (square symbols and circle symbols). Very small values of N_{mg}, however, exclude close points in subsequent growths (cross symbols), hence leading to a higher total number of growths.

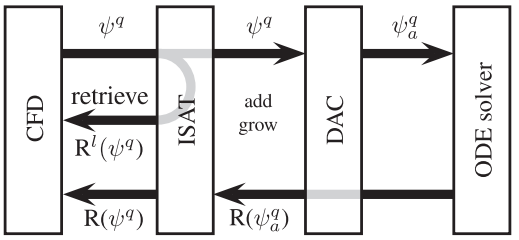

Fig. 2. The TDAC method. The ISAT algorithm try to retrieve the mapping $R^l(\psi^q)$ of the query composition ψ^q. In case of additions and growths, DAC simplifies the mechanism at runtime before providing the composition with active species ψ^q_a to the stiff ODE solver to compute the mapping $R(\psi^q_a)$. This mapping is then extended by ISAT to the full composition space $R(\psi^q)$.

of the EOA (the stored composition). Then, even if part of the following queries are in the EOA, part of them require additional growths as shown by the square and circle symbols in Fig. 1. In this case, replacing the stored composition centered at ψ^0 by the one centered at ψ^q is more efficient.

On the other hand, very small values of N_{mg} stop reducing the total number of growths, but instead increase it dramatically. This is due to the initial conservative description of the EOA. When a EOA is created, it is usually grown to include many other close points. But if it is replaced more often, a lot of points included after few growths are then excluded. This is illustrated by the cross symbols in Fig. 1.

Values for N_{ms} and N_{mg} in the context of HCCI simulations are given in the results section along with a sensitivity analysis.

As the stored points are useless after a few timesteps, the total size of the binary tree can be strongly limited (around 1000 leafs) without any loss of efficiency. Furthermore, this limited size allows faster retrieves and avoids memory issue when using very large mechanisms. Once the maximal number of points is reached, the tree is cleared and repopulated with the use of a most recently used list.

In ICE simulations, the constant pressure assumption is not valid, therefore, the current implementation also stores the pressure.

2.4. TDAC: coupling of ISAT and DAC

The number of operations required for solving the chemical kinetics in CFD simulations depends on the number of cells in the mesh and the size of the oxidation mechanism. The number of cells gives the number of time the ODE system will be integrated. The size of the mechanism defines the level of complexity to integrate the system of stiff nonlinear ODE. Reduction of the computational effort for these separated aspects is achieved by the TDAC method, coupling ISAT and DAC. The ISAT algorithm intends to reuse previously computed results, hence decreasing the effect of the number of cells, whereas the DAC method finds a skeletal mechanism at runtime, hence reducing the effect of the mechanism size. The coupling can be visualized as successive layers (see Fig. 2): when ISAT receives a query ψ^q that needs to integrate the ODE set (growth and addition operations), it provides ψ^q to the DAC algorithm which then find the reduced mechanism for the local thermochemical conditions and provides the reduced set of active species ψ^q_a to the stiff ODE solver. This solver computes the reaction mapping for the reduced set $R(\psi^q_a)$ that is used by ISAT to build the reaction mapping $R(\psi^q)$ in the full composition space. Using simplification methods at distinct levels combines their effects and allows a significant reduction of the computational cost as shown in the next section.

The coupling with the DAC method requires ISAT to manipulate and store chemical points in a composition space with variable dimensions, i.e., with variable active species. Therefore, ISAT stores the mapping of the active species but new variables are introduced to extend the mapping to the full composition space when retrieving or growing points.

It may not be necessary to add new points to the binary tree when the number of active species changes. Therefore, the EOA needs to be checked and grown in the full composition space. Because **A** is computed through the Jacobian, when the number of species is reduced, it only takes active species into account and is more compact. To include inactive species in the definition of the EOA, the method uses an extended **A**. This matrix includes the lines of the identity matrix corresponding to the inactive species index as if the reaction mapping was computed with Eq. (1) in the full composition space.

3. Results

This section first analyses the performance of TDAC compared to direct integration, ISAT

Please cite this article in press as: F. Contino et al., *Proc. Combust. Inst.* (2010), doi:10.1016/j.proci.2010.08.002

and DAC in simplified 2D HCCI cases using *n*-heptane mechanisms. Then, the method is validated in a real HCCI engine case using a detailed 857-species iso-octane mechanism. Finally, an approximation of the speed-up factor for this case is proposed.

3.1. Performance of TDAC

The performance of TDAC has been evaluated on a simplified 2D geometry to get direct integration results of the full HCCI cycle in workable time. The solver used to integrate the system of ODE is based on the semi-implicit mid-point rule developed by Bader and Deuflhard [28]. Four meshes with numbers of cells ranging from 63 to 374 at top dead center (TDC) have been used (the total number of cells changes during simulations because the dynamic mesh layering technique is used). To analyze the effect of the mechanism size, four *n*-heptane mechanisms with increasing number of species have been used: the 44-species skeletal mechanism of Liu et al. [29], the 159- and 282-species reduced mechanism of Seiser et al. [30] and the 561-species detailed mechanism of Curran et al. [31,32].

The results of TDAC and direct integrations are in very good agreement as shown in Fig. 3a and b.

The achieved speed-up factors are illustrated in Table 1 as a function of the number of mesh cells and chemical species when ISAT, DAC and TDAC are used.

The efficiency of ISAT depends on the level of inhomogeneity and the range of thermochemical conditions. For homogeneous thermochemical conditions, most of the queries are retrieved by ISAT, which requires $O(1)$ direct integrations. When completely inhomogeneous and unsteady, most of the queries result in additions or growths, hence requiring $O(N_{\text{cell}})$ direct integrations. In the HCCI test case, the system is unsteady but rather homogeneous which explains that, compared to direct integrations performed in every cells, the speed-up obtained with TDAC is a linear function of the number of cells (see Fig. 4 where the values for the four mechanisms are normalized by the data of the mesh with 63 cells).

The contribution of DAC is highlighted by the use of various mechanisms. In one cell, the direct integration of the reaction equations requires $O(N_s^2)$ operations. On the other hand, DAC requires $O(N_r)$ operations [22]. As the number of reactions is proportional to the number of species [33], the speed-up of the TDAC method is then proportional to N_s as shown in Fig. 5. On this figure, the values are normalized by the results obtained on each meshes using the 44-species mechanism.

When ISAT and DAC are combined in TDAC, the achieved speed-up factor is influenced by the total number of retrieves, the number of species to be considered for each cell and the computational overheads required to dynamically reduce the chemical mechanism. This explains the similar performances between ISAT and

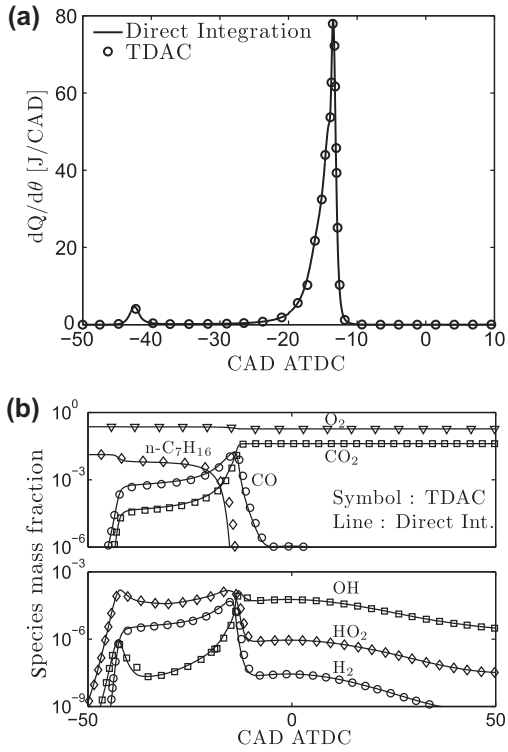

Fig. 3. (a) Heat release rate and (b) species mass fraction for direct integration (line) and TDAC (symbol) on the HCCI simplified geometry with 374 cells using the 159-species mechanism.

Table 1
Speep-up factor obtained for the simplified 2D HCCI cases.

		N_{cell}			
		63	154	252	374
$N_s = 44$	TDAC	5.5	8.4	9.1	9.6
	ISAT	5.7	9.0	9.1	12
	DAC	1.1	1.2	1.1	1.0
$N_s = 159$	TDAC	15	19	24	28
	ISAT	12	13	16	16
	DAC	2.9	2.9	2.8	3.2
$N_s = 282$	TDAC	27	37	40	56
	ISAT	13	17	19	28
	DAC	5.3	4.9	4.8	5.0
$N_s = 561$	TDAC	50	105	110	150
	ISAT	6.5	9.0	8.7	13
	DAC	29	32	28	26

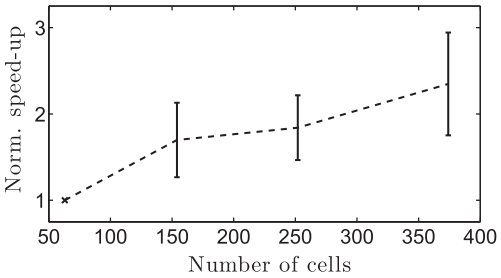

Fig. 4. Range of speed-up for the four mechanisms normalized by the results obtained on the mesh with 63 cells. In these low inhomogeneity cases, the speed-up using TDAC is proportional to the number of cells.

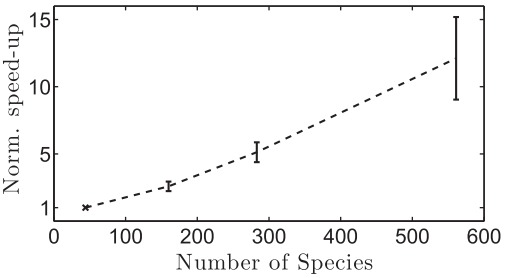

Fig. 5. Range of speed-up for the four meshes normalized by the results obtained using the 44-species mechanism. The direct integration requires $O(N_s^2)$ operations while $O(N_s)$ operations are needed by DAC. Accordingly, the speed-up factor using TDAC increases linearly with the number of species.

TDAC when a low number of cells is used and the very high speed-up factors of TDAC with refined meshes and very complex mechanisms as it can be seen for the mesh with 374 cells, where the speed-up factor ranges from 9.6 with 44 species to 150 with 561 species (see Table 1).

In most HCCI cases, a value of N_{ms} between 0.5 and 1.0 crank angle degree (CAD) is sufficient to properly match the pressure trace computed with direct integration. Below these values, there is a very small impact on the error ε_p defined by:

$$\varepsilon_p = \frac{1}{K p_{max}} \sum_{i=1}^{K} |p_{i,\mathrm{TDAC}} - p_{i,\mathrm{DI}}|, \qquad (5)$$

where K is the number of time steps, the pressures p are volume averaged over the whole domain and the subscript "*max*" denotes the maximum pressure during the whole simulation (see Fig. 6a).

As described in the previous section, the use of N_{mg} reduces the total number of growths. The optimal value for this configuration is around 20 where the total number of growths is reduced below 3000 compared to 5000 without N_{mg}. Very small values, however, increase dramatically the total number of growths (see Fig. 6b). As the

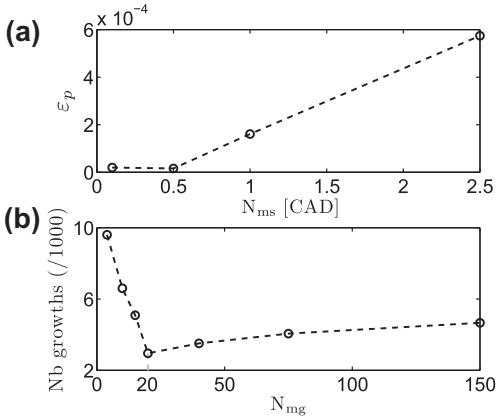

Fig. 6. For the mesh with 374 cells and the 159-species mechanism, (a) mean error on the pressure ε_p as a function of N_{ms} and (b) the total number of growth as a function of N_{mg}.

EOA is distorted either by growth from inhomogeneities in the same time-step or from rather homogeneous successive time-step, the optimal value for N_{mg} mainly depends on the type of application. In HCCI simulations, this value is around 5% of the total number of cells.

3.2. Experimental validation

The experimental validation has been performed according to the extensive data on low load HCCI combustion obtained on a medium-duty diesel engine (displacement of 0.98 l/cylinder) by Hessel et al. [34]. The mesh follows the specifications given by the authors: axi-symmetric with a flat cylinder head, without valves, with a gasket and a crevice zone and it has 12,000 cells at TDC. The simulations use the detailed 857-species iso-octane mechanism of Curran et al. [31]. They are performed from inlet valve closing to exhaust valve opening. The temperature wall function of Han and Reitz [35] is used to compute the wall heat transfer and the RNG k–ε model modified by Han and Reitz [36] is used for the turbulence. Initial and boundary conditions for different equivalence ratios ϕ can be found in Table 2.

For all simulated conditions, the agreement between the computed and experimental results are very good for both the auto-ignition time and the maximum cylinder pressure (see Fig. 7). A rather good agreement is observed for the predicted emissions which slightly overestimates the unburnt fuel and the CO to CO_2 conversion (see Fig. 8a and b) while maintaining correct trends. The mechanism used for iso-octane oxidation kinetics has been extensively validated for a large range of combustion conditions. As we have

Please cite this article in press as: F. Contino et al., *Proc. Combust. Inst.* (2010), doi:10.1016/j.proci.2010.08.002

Table 2
Initial and boundary conditions based on Hessel et al. [34] for different equivalence ratios ϕ. Temperatures are in K, pressures in bar and species concentrations in mass fraction.

	ϕ				
	0.12	0.16	0.20	0.24	0.28
p	1.367	1.361	1.378	1.377	1.371
T_{gas}	467.8	468.6	464.1	465.0	463.2
T_{liner}	381.4	382.4	383.5	384.4	385.3
T_{head}	399.8	403.0	406.5	409.6	412.5
T_{piston}	426.6	433.0	440.0	446.2	451.9
iC_8H_{18}	0.00759	0.01012	0.01265	0.01519	0.01774
O_2	0.22932	0.22824	0.22723	0.22633	0.22547
CO_2	0.00097	0.00157	0.00220	0.00250	0.00274
H_2O	0.00060	0.00073	0.00082	0.00092	0.00102
CO	0.00053	0.00034	0.00008	0.00003	0.00002

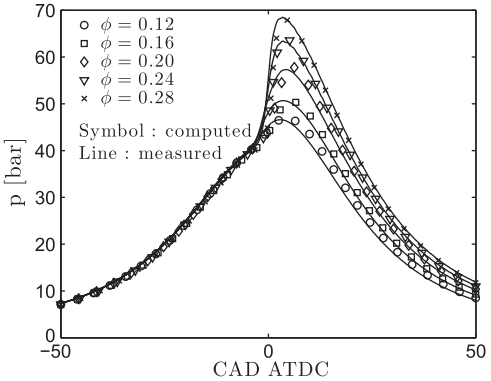

Fig. 7. Pressure traces for computed (symbol) and measured (line) [34] data of the HCCI engine cycle.

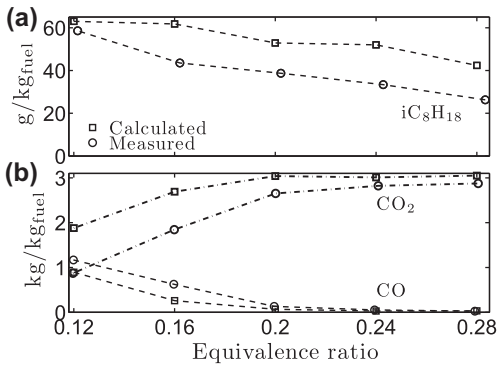

Fig. 8. Engine emissions [34] data: (a) unburnt fuel and (b) CO_2 and CO as a function of the equivalence ratio.

shown in the previous section that TDAC and direct integration of the system are in good agreement and as the influence of the wall temperature and shape on the engine emissions is very important (illustrated in details in [37]), these discrepancies are mainly due to the uncertainties on the wall temperature and the model assumptions for the crevice and gasket regions (heat transfer, turbulence model, mesh refinements, etc.).

For single adiabatic cells, Liang et al. observed that, after the main combustion stage, the number of active species dropped to a value around 30, for the burned gas reactions [14]. In the present case, due to wall heat transfer the conversion to burned gas is not complete near the wall and the algorithm retains more active species (around 250).

A higher number of cells, especially near the wall, corresponds to an increase of the level of inhomogeneity, hence a more severe tolerance ε_{ISAT} is required. A value of 10^{-4} is commonly used but lower values (around 10^{-5}) are required for more inhomogeneous cases. On practical meshes, the inhomogeneity is increased because of the level of details required, i.e., to model the heat transfer near the walls. Therefore, the efficiency of the ISAT algorithm is below what could be expected by extrapolating the results of Table 1.

The value of the speed-up factor for the real engine case, reported in the experimental validation, cannot be directly computed. It is approximated according to the average computational time required by direct integration for one cell, multiplied by the number of queries the solver would receive in the course of the simulation. For 4×10^7 queries and an average time of 2.4 s on a single CPU, the direct integration would require more than 3 years compared to 86 h using TDAC. This approximation yields a more than 300-fold computational time reduction. This factor is well above what was previously reported for HCCI simulations using ISAT (up to 10 see [26]) and for single-cell simulations using DAC (between 15 and 70 depending on the mechanism [14,21]).

4. Conclusion

A new method termed tabulation of dynamic adaptive chemistry (TDAC) which combines the advantages of ISAT and DAC has been

Please cite this article in press as: F. Contino et al., *Proc. Combust. Inst.* (2010), doi:10.1016/j.proci.2010.08.002

developed. The principle of TDAC is to apply simplification methods on separate steps of the combustion calculation. These methods allow the speed-up to grow linearly with the number of species and the number of cells in the mesh. Even if the inhomogeneity observed in practical cases limits the speed-up due to less retrieves of the ISAT algorithm, a significant speed-up factor of about 300 is achieved compared to direct integration in the context of HCCI engine simulations. For this reason, TDAC represents a promising solution for CFD simulations including detailed mechanisms that are inconceivable using direct integration. The methodology can also be applied to the simulation of other combustion systems such as Diesel engines and gas turbine combustors.

Acknowledgment

Funding of the F.R.S. – FNRS is gratefully acknowledged.

References

[1] C.K. Westbrook, W.J. Pitz, O. Herbinet, H.J. Curran, E.J. Silke, *Combust. Flame* 156 (2009) 181–199.
[2] S. Kong, Y. Sun, R.D. Reitz, *J. Eng. Gas Turbines Power* 129 (2007) 245–251.
[3] F.M.C. Gauding, B. Kerschgens, A. Vanegas, H.W. Won, N. Peters, C. Hasse, *SAE Paper* 2009-01-0720, 2009.
[4] M. Singer, S. Pope, *Combust. Theor. Model.* 8 (2004) 361–383.
[5] T. Lu, C.K. Law, *Prog. Energy Combust. Sci.* 35 (2009) 192–215.
[6] S.B. Pope, *Combust. Theor. Model.* 1 (1997) 41–63.
[7] J.B. Bell, N.J. Brown, M.S. Day, et al., *Proc. Combust. Inst.* 28 (2000) 107–113.
[8] U. Maas, S.B. Pope, *Combust. Flame* 88 (1992/3) 239–264.
[9] O. Gicquel, N. Darabiha, D. Thèvenin, *Proc. Combust. Inst.* 28 (2000) 1901–1908.
[10] A.S. Tomlin, M.J. Pilling, T. Turányi, J.H. Merkin, J. Brindley, *Combust. Flame* 91 (1992) 107–130.
[11] A. Massias, D. Diamantis, E. Mastorakos, D.A. Goussis, *Combust. Flame* 117 (1999) 685–708.
[12] T. Lu, C.K. Law, *Proc. Combust. Inst.* 30 (2005) 1333–1341.
[13] P. Pepiot-Desjardins, H. Pitsch, *Combust. Flame* 154 (2008) 67–81.
[14] L. Liang, J.G. Stevens, J.T. Farrell, *Proc. Combust. Inst.* 32 (2009) 527–534.
[15] S.S. Ahmed, F. Mauss, G. Moréac, T. Zeuch, *PCCP* 9 (2007) 1107–1126.
[16] T. Zeuch, G. Moréac, S.S. Ahmed, F. Mauss, *Combust. Flame* 155 (2008) 651–674.
[17] N. Peters, *Reduced Kinetic Mechanisms and Asymptotic Approximations for Methane–Air Flames*, 1991, pp. 48–67.
[18] H. Weller, G. Tabor, H. Jasak, C. Fureby, *J. Comput. Phys.* 12 (1998) 620–631.
[19] T. Lucchini, G. D'Errico, F. Brusiani, G.M. Bianchi, *Proceedings of the COMODIA 2008 Conference*.
[20] G. D'Errico, D. Ettorre, T. Lucchini, *SAE Int. J. Fuel Lubricants* 1 (2009) 452–465.
[21] L. Liang, J.G. Stevens, S. Raman, J.T. Farrell, *Combust. Flame* 156 (2009) 1493–1502.
[22] T. Lu, C.K. Law, *Combust. Flame* 144 (2006) 24–36.
[23] L. Lu, S.B. Pope, *J. Comput. Phys.* 228 (2009) 361–386.
[24] S.B. Pope, *Algorithms for Ellipsoids*, Technical Report FDA-08-01, Cornell University, 2008.
[25] W.H. Press, S.A. Teukolsky, W.T. Vetterling, B.P. Flannery, *Numerical Recipes: The Art of Scientific Computing*, third ed., Cambridge University Press, 2007.
[26] M. Embouazza, D.C. Haworth, N. Darabiha, *SAE Paper* 2002-01-2773, 2002.
[27] I. Veljkovic, P.E. Plassmann, D.C. Haworth, *ICCSA (1)*, pp. 643–653.
[28] G. Bader, P. Deuflhard, *Numer. Math.* 41 (1983) 373–398.
[29] S. Liu, J.C. Hewson, J.H. Chen, H. Pitsch, *Combust. Flame* 137 (2004) 320–339.
[30] R. Seiser, H. Pitsch, K. Seshadri, W.J. Pitz, H.J. Gurran, *Proc. Combust. Inst.* 28 (2000) 2029–2037.
[31] H.J. Curran, P. Gaffuri, W.J. Pitz, C.K. Westbrook, *Combust. Flame* 129 (2002) 253–280.
[32] H.J. Curran, P. Gaffuri, W.J. Pitz, C.K. Westbrook, *Combust. Flame* 114 (1998) 149–177.
[33] C.K. Law, *Proc. Combust. Inst.* 31 (2007) 1–29.
[34] R.P. Hessel, D.E. Foster, S.M. Aceves, et al., *SAE Paper* 2008-01-0047, 2008.
[35] Z. Han, R.D. Reitz, *Int. J. Heat Mass Transfer* 40 (1997/2) 613–625.
[36] Z. Han, R.D. Reitz, *Combust. Sci. Technol.* 106 (1995) 267–295.
[37] J.B. Heywood, *Internal Combustion Engine Fundamentals*, McGraw-Hill, 1988.

Please cite this article in press as: F. Contino et al., *Proc. Combust. Inst.* (2010), doi:10.1016/j.proci.2010.08.002